Ferritin Nanocages with Biologically Orthogonal Conjugation for Vascular Targeting and Imaging

Makan Khoshnejad[†,*,#], Colin F. Greineder[†,*,#,¶], Katherine W. Pulsipher[§], Carlos H. Villa[†], Burcin Altun[‖], Daniel C. Pan[†], Andrew Tsourkas[‖,¶], Ivan J. Dmochowski[§,¶], Vladimir R. Muzykantov[*,†,¶]

Supplementary Figures

a)

Residue	Amino Acid	Side Chain SASA (Å²)	Ratio (%)
2	Ser	85.78	100
5	Ile	75.11	51
9	Tyr	0.0	0
79	Phe	96.53	53.6
83	Lys	131.54	80
105	Lys	131.15	68.8
112	Leu	80.47	55
155	Leu	48.07	32.9

b)

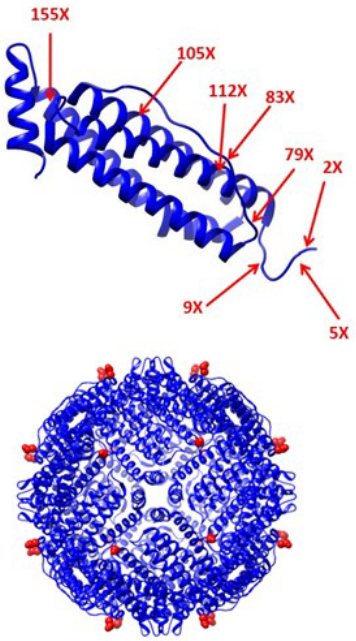

Figure S1 Generation of FTL-X variant library. a) Solvent accessible surface area (SASA) analysis of hFTL. The table shows the characteristics of the eight residues selected for uAA incorporation. The final column shows the ratio of each side chain SASA and a "random coil" value for that amino acid, with a value of greater than 50% indicating a relatively solvent exposed amino acid[44]. b) Structure of human ferritin light chain 24mer and monomer. Azidophenylalanine was genetically incorporated into different amino acid positions (indicated in red) for determining the optimal AzF position suitable for conjugation.

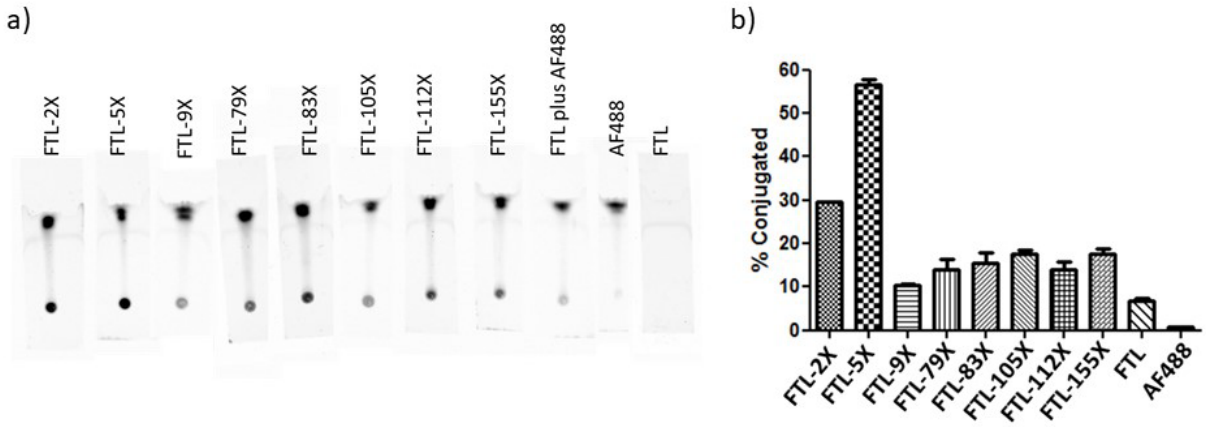

Figure S2 Evaluation of FTL-5X variant conjugation efficiency. a) Thin layer chromatography was used for analysis of conjugation efficiency of FTL-X variants to DBCO-Alexafluor488. As shown in b) the percent fluorophore conjugated was the highest for FTL-5X at 57%.

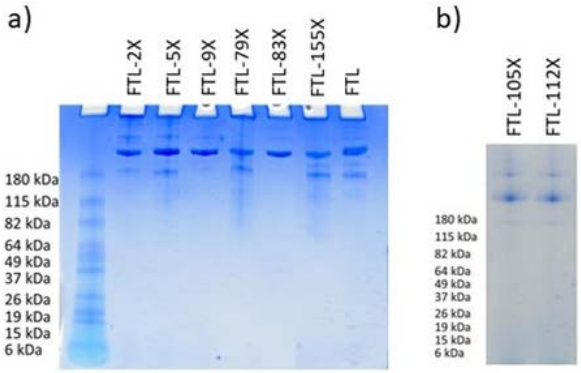

Figure S3 Native PAGE analysis of FTL-X variants. Native PAGE of a) FTLX-2, -5, -9, -79, -83, -155, and wild type human FTL, and b) FTLX-105, and -112 variants.

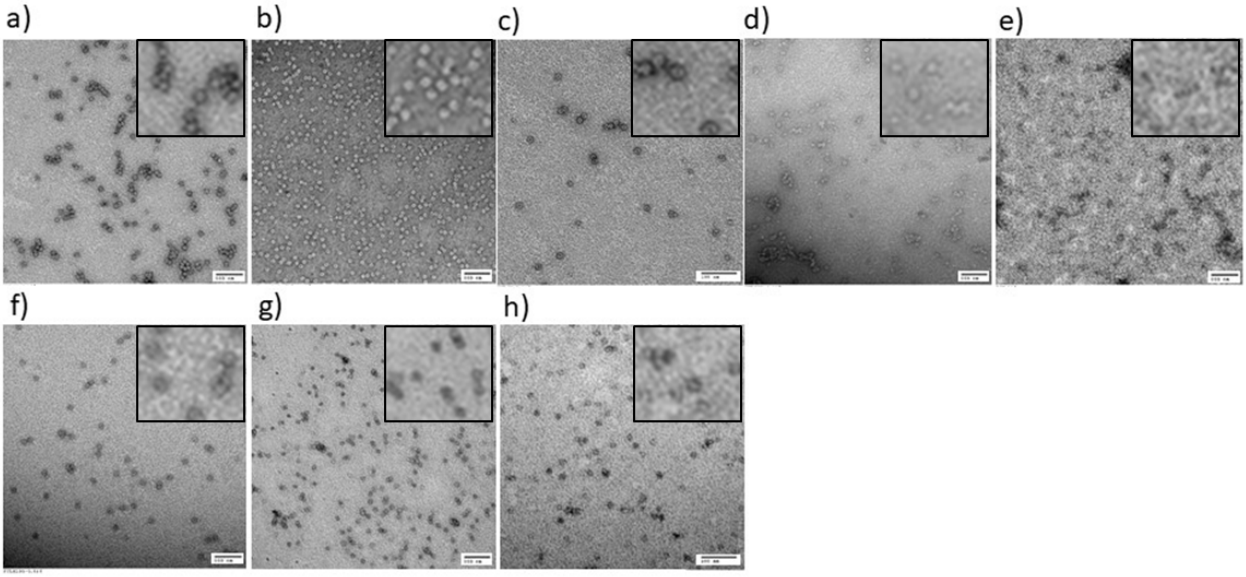

Figure S4 Transmission electron microscope (TEM) analysis of FTL-X variants. TEM images of a) FTL-2X, b) FTL-5X, c) FTL-9X, d) FTL-79X, e) FTL-83X, f) FTL-105X, g) FTL-112X, and h) FTL-155X. Scale bar: 100 nm.

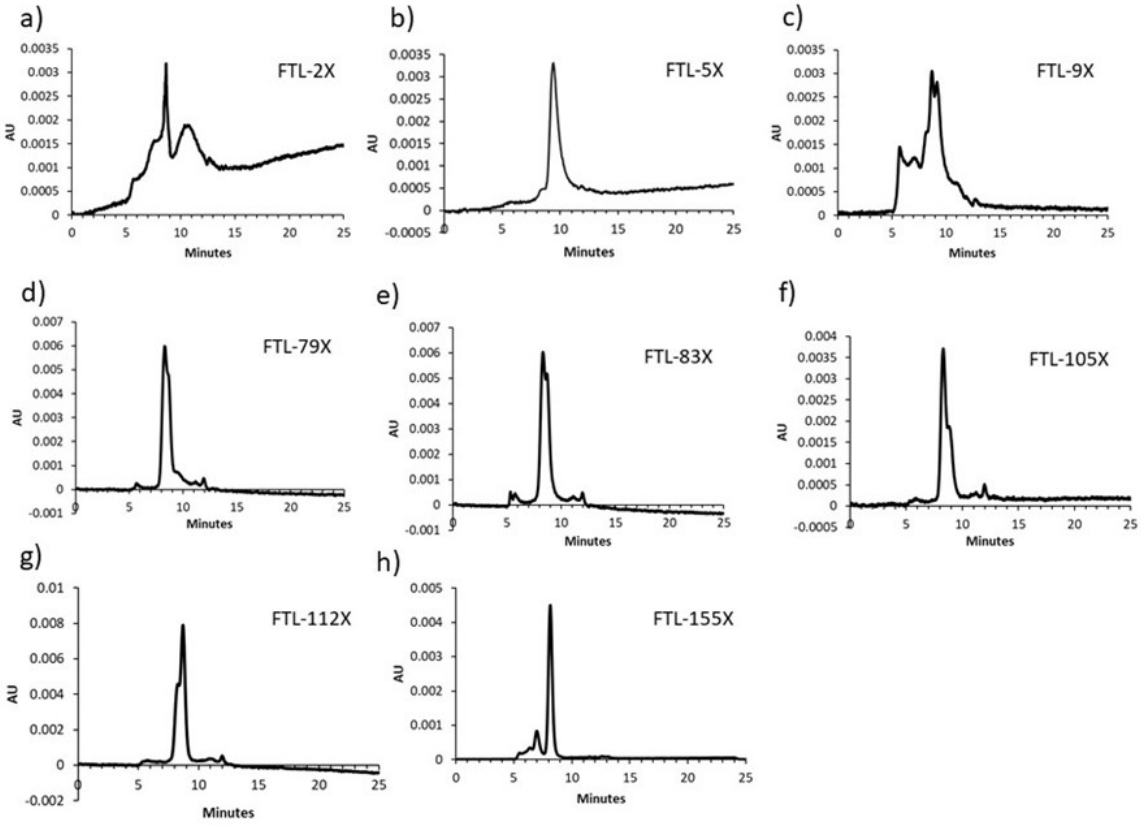

Figure S5 HPLC analysis of FTL-X variants. HPLC absorbance trace of a) FTL-2X, b) FTL-5X, c) FTL-9X, d) FTL-79X, e) FTL-83X, f) FTL-105X, g) FTL-112X, and h) FTL-155X.

Samples were analyzed using BioSep SEC-s3000 column by isocratic method with 100% PBS, pH 7.4.

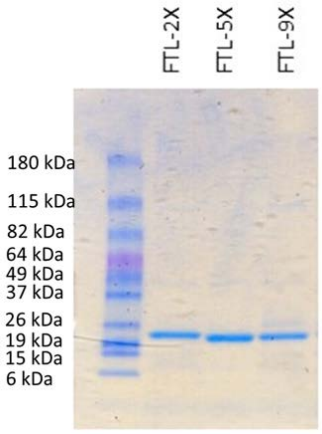

Figure S6 Denaturing SDS-PAGE analysis of FTL-X variants. Denaturing SDS-PAGE analysis of FTL-2X, -5X, and -9X variants.

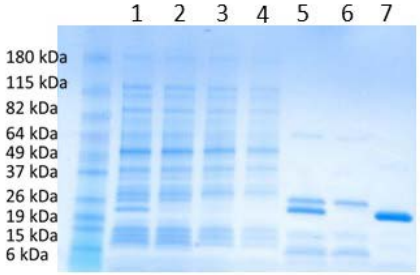

Figure S7 SDS-PAGE analysis of FTL-5X. SDS-PAGE analysis was performed on a) FTL-5X from bacterial lysates and purified fractions. Lane numbers indicate the following: 1) FTL-5X (+AzF) whole lysate, 2) FTL-5X (-AzF) whole lysate, 3) FTL-5X (+AzF) post-sonication pellet, 4) FTL-5X (-AzF) post-sonication pellet, 5) FTL-5X (+AzF) supernatant, 6) FTL-5X (-AzF) supernatant, and 7) FTL-5X (+AzF) elution.

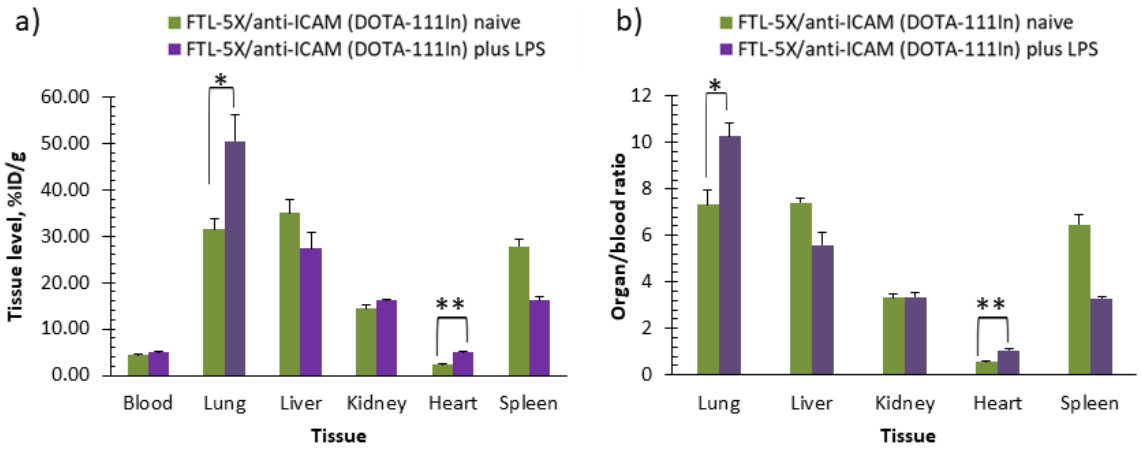

Figure S8 ***In vivo*** **targeting of ^{111}In-labeled targeted FTL-5X to ICAM-1.** a) Biodistribution of ^{111}In-DOTA-labeled FTL-5X conjugated to anti-ICAM in naive and LPS-treated mice at 30 min. Tissue uptake is indicated as mean ± SEM (n=3). b) Localization ratio of selected organs. Significant differences determined by t-test with Bonferroni correction to account for multiple comparisons (*p < 0.05, **p <0.01).

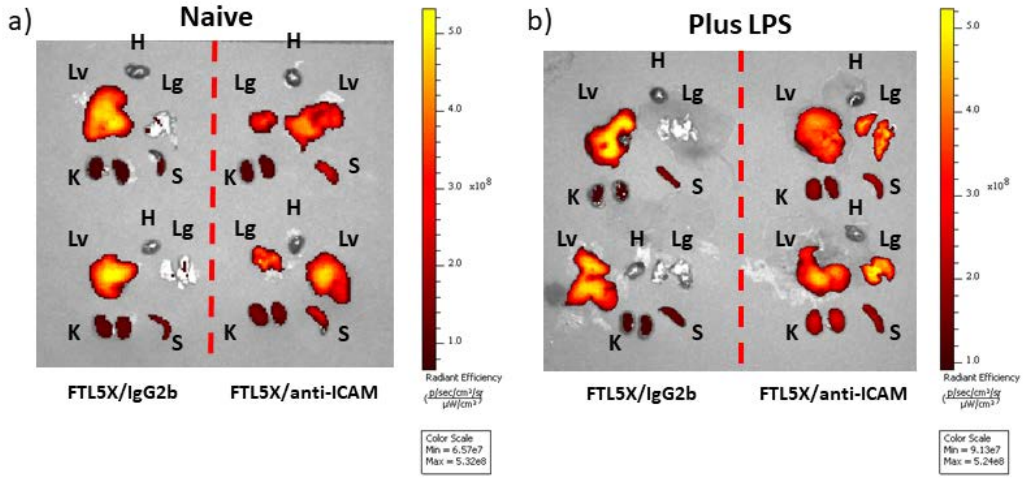

Figure S9 Near-infrared imaging of organs harvested from mice treated with targeted FTL-5X. *Ex vivo* imaging of organs treated with AF750-labeled FTL-5X conjugated to anti-ICAM and IgG2b isotype control in a) naive and b) LPS-treated mice at 30 min.

Radiant Efficiency [p/s/cm2/sr]/[μW/cm2]					
	Liver	Lung	Kidney	Heart	Spleen
FTL5X/IgG naive	1.43E+10 ± 1.75E+09	1.88E+09 ± 1.02E+08	2.67E+09 ± 2.48E+08	7.04E+08 ± 8.75E+06	1.35E+09 ± 1.66E+08
FTL5X/IgG plus LPS	1.58E+10 ± 6.90E+08	2.12E+09 ± 7.50E+07	2.50E+09 ± 9.95E+07	6.83E+08 ± 2.53E+07	1.67E+09 ± 3.40E+07
FTL5X/anti-ICAM naive	1.15E+10 ± 1.75E+08	4.02E+09 ± 4.84E+08	2.82E+09 ± 2.85E+08	7.06E+08 ± 1.98E+07	2.00E+09 ± 6.00E+06
FTL5X/anti-ICAM plus LPS	1.46E+10 ± 1.44E+09	6.91E+09 ± 2.84E+08	3.73E+09 ± 5.35E+08	7.02E+08 ± 2.96E+07	2.05E+09 ± 1.15E+08

Table S1 Fluorescence intensity of near-infrared imaged organs harvested from mice treated with targeted FTL-5X. Radiant efficiency of e*x vivo* imaged organs from mice treated with AF750-labeled FTL-5X conjugated to anti-ICAM and IgG2b isotype control in naive and LPS treated mice at 30 minutes.

a) Tissue level, %ID/g						
	Blood	Lung	Liver	Kidney	Heart	Spleen
FTL5X/IgG2b naive	11.46 ± 0.55	3.48 ± 0.14	28.39 ± 2.34	5.67 ± 0.14	1.95 ± 0.16	99.56 ± 10.74
FTL5X/IgG2b plus LPS	9.94 ± 0.56	2.89 ± 0.57	18.15 ± 1.54	4.34 ± 0.56	1.45 ± 0.18	53.72 ± 11.32
FTL5X/anti-ICAM naive	2.98 ± 0.06	43.30 ± 6.99	17.01 ± 1.36	9.04 ± 0.70	2.62 ± 0.23	30.24 ± 3.66
FTL5X/anti-ICAM plus LPS	3.48 ± 0.23	84.44 ± 12.89	12.67 ± 1.57	8.81 ± 0.50	3.47 ± 0.46	19.70 ± 3.13

b) Organ/blood ratio					
	Lung	Liver	Kidney	Heart	Spleen
FTL5X/IgG2b naive	0.30 ± 0.01	2.61 ± 0.25	0.50 ± 0.03	0.17 ± 0.01	8.68 ± 0.80
FTL5X/IgG2b plus LPS	0.29 ± 0.05	1.85 ± 0.25	0.43 ± 0.03	0.15 ± 0.01	5.35 ± 0.89
FTL5X/anti-ICAM naive	14.71 ± 2.78	5.94 ± 0.34	3.12 ± 0.21	0.91 ± 0.08	10.19 ± 1.39
FTL5X/anti-ICAM plus LPS	23.91 ± 6.98	3.50 ± 0.29	2.45 ± 0.07	0.88 ± 0.04	5.68 ± 0.73

Table S2 Biodistribution of ^{125}I-labeled targeted FTL-5X to ICAM-1. a) Tissue levels (%ID/g) and b) Organ/blood ratio of ^{125}I-labeled targeted FTL-5X nanoparticles in naive and LPS-treated mice at 30 min. Tissue uptake is indicated as mean ± SEM.